ADVANCED MATERIALS INTERFACES
Open Access
www.advmatinterfaces.de

Antimicrobial Personal Protection Clothing: Development of Visible Light Activated Antimicrobial Coatings for Nonwoven Polypropylene Fibers

*Jean Michél Merkes, Tarushyam Mukherjee, Silvia Chiera, Olli-Ville Laukkanen, Joerg Bruenke, Tim Brust, Francesco Tessarolo, Fabian Kiessling, Magnus Rueping, and Srinivas Banala**

During the COVID-19 pandemic, the use of polypropylene fleece-based personal protection equipment (PPE) increased significantly to over ten million tons. Typically, most PPEs are discarded after a single use, to prevent self-infection of users and spread of infectious agents. However, in order to minimize plastic waste without compromising the protective properties of PPE, it is crucial to explore new reusable or longer-lived materials. Here, a visible light-activatable antimicrobial photodynamic dye coating for PPEs is presented. In this context, coating with thiomorpholino-methylene blue (TMB), derived from methylene blue by introducing two thiomorpholine units, is found to show high antibacterial activity. TMB is integrated into rotary printing suspension, a commercial nitrocellulose-based printing matrix. The concentration of TMB in adhesive is optimized, and found that 5% TMB is suitable for coating PPE, for reducing the number of Gram-positive and -negative bacteria by 99.99% after 6 h of white light irradiation. Bacterial filtration efficiency and breathability tested according to EN 14683, confirmed that TMB coating does not affect the filter performance. Thus, this antimicrobial photodynamic dye coating technique offers a promising solution for a safer and extended use of PPE, and reduction of plastic waste generated by PPEs.

1. Introduction

Personal protection equipment (PPE, e.g., surgical masks, head caps, gowns, and coveralls) aims to prevent transmission of infections in healthcare settings.[1] Respiratory masks like N95, FFP2, FFP3, and multi-layered surgical masks can filter out aerosolized droplets of a certain size and prevent airborne pathogens from entering the host. However, prolonged use of surgical masks is not recommended, due to concerns of surface contamination, reduced efficiency in respiratory protection, or self-infection due to increased concentration of pathogens on the mask surface.[2] Since the onset of the COVID-19 pandemic in 2020, an increased use of PPEs in all medical facilities resulted in a drastic rise in the amount of PPE used and waste generated.

Polypropylene is a widely used thermoplastic polymer for fiber creation for PPE.

J. M. Merkes, T. Mukherjee, F. Kiessling, S. Banala
Institute for Experimental Molecular Imaging
RWTH Aachen University Clinic
Forckenbeckstraße 55, 52074 Aachen, Germany
E-mail: srinivas.banala@oc.rwth-aachen.de; sbanala@ukaachen.de
J. M. Merkes, F. Kiessling, S. Banala
Fraunhofer Institute for Digital Medicine MEVIS
Max-Von-Laue-Straße 2, 28359 Bremen, Germany

S. Chiera, F. Tessarolo
Department of Industrial Engineering
University of Trento
Trento 38123, Italy
O.-V. Laukkanen
VTT Technical Research Centre of Finland Ltd
Koivurannantie 1, Jyväskylä 40400, Finland
J. Bruenke
Dr. Bruenke MTC e.K.
Microbiological Testing Competence
Valznerweiherstr. 15, 90480 Nürnberg, Germany
T. Brust
Ultratex GmbH
Lukasstraße 20, 52070 Aachen, Germany
M. Rueping
KAUST Catalysis Centre
King Abdullah University of Science and Technology (KAUST)
Thuwal 23955-6900, Saudi Arabia

The ORCID identification number(s) for the author(s) of this article can be found under https://doi.org/10.1002/admi.202300601

DOI: 10.1002/admi.202300601

Polypropylene is derived from propylene monomer, obtained from petrochemical raw materials, under chain-growth polymerization.[3] The global market volume of it reached 75.57 million tons in 2021, and is projected to reach 100 million tons by 2029.[4] Unfortunately, a significant amount of it ends up in plastic waste, and the COVID-19 pandemic alone contributed to 8.4 ± 1.4 million tons of waste plastics as of August 2021, mostly comprising of PP.[5] Further, ≈25.9 ± 3.8 thousand tons of it ended up in the oceans. During the peak of the pandemic, an estimated 129 billion masks were discarded each month, contributing to a significant increase in waste.[6]

Amidst the COVID pandemic, a project was launched to combat the increasing amount of waste generated by PPE. The project involved integrating light-activated (photodynamic) antimicrobial materials (LAAM) in rotary-printed masks and PPE clothing. The LAAM surfaces enable self-decontamination of PPE under standard household light irradiation. This approach allows the longer usage and reusability of PPEs without compromising its effectiveness, ultimately contributing to the reduction of PPE waste.

LAAM surfaces, decorated either with metal nanoparticles (NP) or organic dyes, generate different types of reactive oxygen species (ROS: $O_2^{\bullet -}$, $HO^{\bullet}$, H_2O_2, $^1O_2$) under light irradiation (for PPEs, preferably visible light). These ROS oxidize a variety of unsaturated molecules and biomolecules, including lipids, proteins, and nucleic acids, leading to cell death. LAAM compounds can be differentiated into two different types, by their ROS producing mechanisms: a) Type 1, by electron transfer to oxygen, yielding superoxide anion ($O_2^{\bullet -}$) or hydroxyl radicals ($HO^{\bullet}$), as well as hydrogen peroxide (H_2O_2), mostly by metal NPs, such as titan dioxide; b) Type 2, by excited state energy transfer to oxygen, yielding singlet oxygen ($^1O_2$) by flipping electron spin, mostly by small organic photosensitizers (PS) dyes.

$^1O_2$ is a highly reactive ROS characterized by an excited state paired electron configuration of $[O_2(^1\Delta_g)]$. It has a lifetime ranging from 86 ms (at 0% humidity) and 54 ms (at 100% humidity), and can diffuse over a few millimeters.[7] The $^1O_2$ oxidizes vital biological molecules, such as aromatic residues in proteins and nucleic acids of living matter, which in turn initiate downstream processes to cause cell death.[8] In terms of the $^1O_2$ generation mechanism, in the first excited state (S1) the PS molecule undergoes an intersystem crossing (ISC), leading to a triplet (T) state (**Figure 1a**). The T-state, upon collision with oxygen ($^3O_2$), transfers energy leading to a change in the valence electron configuration of oxygen from unpaired to a single paired state (see MO diagram in Figure 1b). The $^1O_2$ generated by the PS then diffuses from the surface, and interacts with living matter causing cell-death (Figure 1c). Unreacted $^1O_2$ converts back to $^3O_2$ with the loss of energy by light emission in the near-infrared window, without any accumulation of reactive species in the environment. Consequently, there is no accumulation of toxic species in the air. In addition, the organic photosensitizer materials are typically less toxic than other anti-bacterial materials, thus, exerting minimal negative environmental impact. Furthermore, in contrast to many antibiotics, there are no reports of bacteria developing resistance against the photodynamic action. Hence incorporating PS-based LAAM modifications into materials serves as a safe alternative compared to other antimicrobial preparations.

In current research, there is a growing interest in equipping textiles with antimicrobial properties, as this can reduce the proliferation of pathogens and the risk of spreading diseases.[9] Among antimicrobial, silver-embedded materials,[10–12] silver nanoparticles,[13–17] and quaternary ammonium salts[18–20] are most widely explored. Additionally, the use of organic photosensitizers (OP) has also been explored.[21–27] Here, applications range from the mitigation of chemical weapons (e.g., oxidation of mustard gas),[28] neutralization of odor substances,[29] antimicrobial wound dressing [30] to face masks.[31] In case of the latter, Hong and Sun investigated a benzophenone modified polymer blend, also containing polypropylene in their polymer scope. They showed under UV light irradiation (365 nm) that benzophenone blends exhibited a high antimicrobial activity against both Gram-positive and negative, *S. aureus* and *E. coli*, strains.[31] However, UV-light is not ideal for wearable PPEs, thus, we want to substitute it with visible light to make continuous sterilization at ambient conditions possible.

2. Results and Discussion

In this study, we investigated the potential of phenothiazine core dyes as printable materials for decorating PPE textile surfaces. The most common representative of phenothiazine dyes is methylene blue (MB, see **Figure 2**), known for its high $^1O_2$ production yields under visible light excitation, which has been used in medicine, for example for treating methemoglobinemia[32] and for cancer photodynamic therapy.[33] However, in our case, the high water-solubility of MB is not suitable, as the dye could ooze out from masks with sweat. Therefore, we explored suitable alternatives, and here we report on the thiomorpholine-modified phenothiazine dye, named thiomorpholino-methylene blue (TMB, see Figure 2), as a printable photosensitizer suitable for PP based PPE textiles.

Considering various modifications available for phenothiazine compounds, we postulated that TMB holds great potential. Due to its increase in molecular weight, by 112 Da with two thiomorpholines, and using iodide as counterion the hydrophobicity of the dye is increased to make it water-insoluble.[34] In 2018 Delport et al. published TMB as a possible monoamine oxidase inhibitor for treating depression.[35] They prepared TMB using an excess of thiomorpholine (also as a base), which increased the cost of the material production. For a cost-effective modification, we used trimethylamine as an additional base with only two equivalents of thiomorpholine in preparing the TMB. This modification yielded TMB in quantitative yields after precipitation in water. The obtained TMB was characterized using NMR, MS, IR, and UV/Vis spectroscopy (see ESI).

Subsequently, the $^1O_2$ generation yield of TMB was measured using red-LED based irradiation and methylene blue (MB) as a reference (**Figure 3**). For this, solutions of photosensitizers in a concentration of 10 µM in DMSO were prepared and ten-fold excess (of 100 µM) of the widely used $^1O_2$ scavenger, 1,3-diphenylbenzofuran (DPBF) was added. The pre-mixed solutions were then irradiated in 96 well-plate with 690 ± 10 nm LED-light source, with a power of 9.27 ± 0.3 Wcm^{-2}.[36] The degradation of the DPBF over the irradiation time was monitored by measuring UV/Vis absorption, for up to 3 min. The experiment showed that the rate of $^1O_2$ production (quantum yield) of TMB

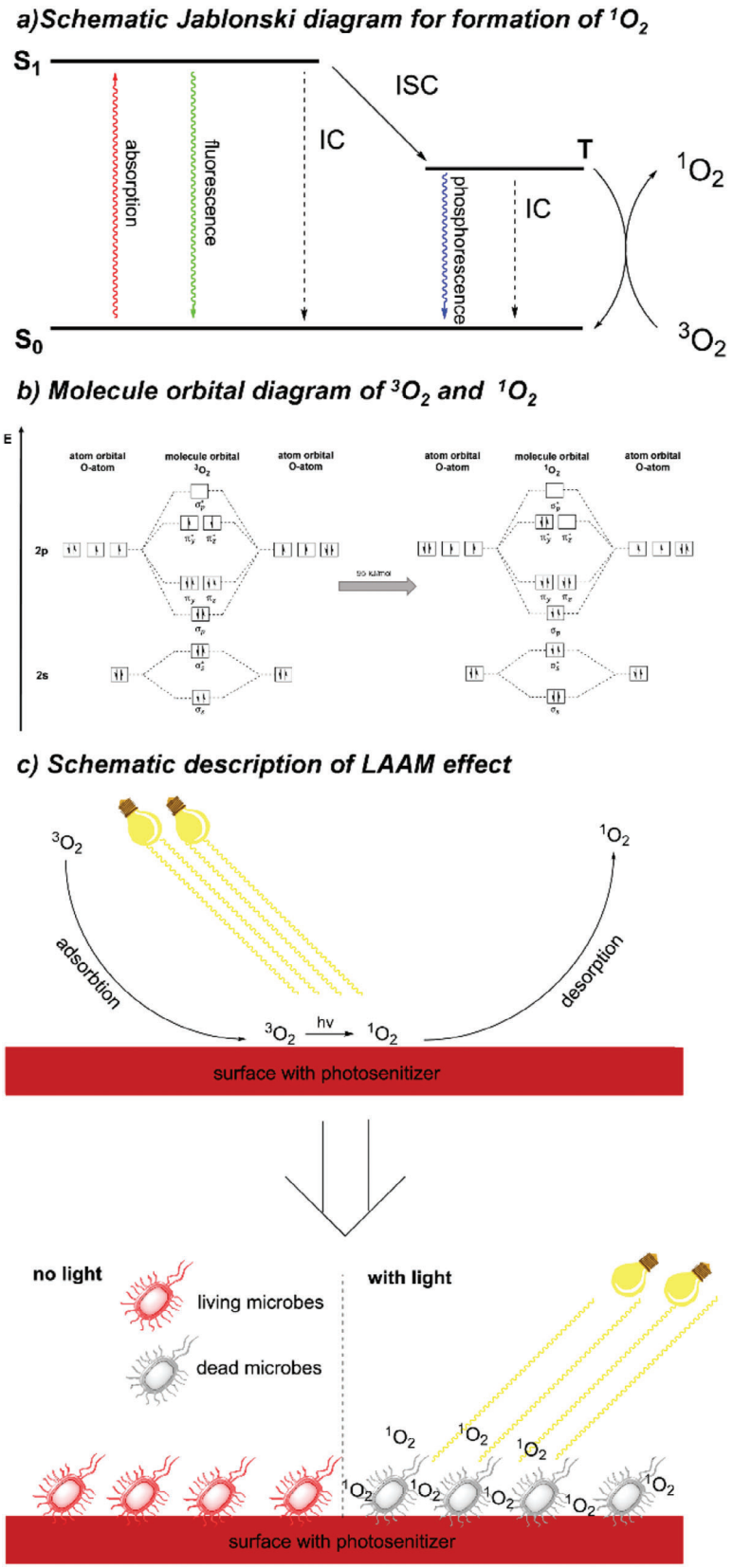

Figure 1. a) A schematic Jablonski diagram for the photophysical pathway of singlet oxygen ($^1O_2$) generation; b) Molecule orbital diagrams of triplet oxygen ($^3O_2$) and $^1O_2$; c) schematic description of the antimicrobial effect on surfaces under light irradiation.

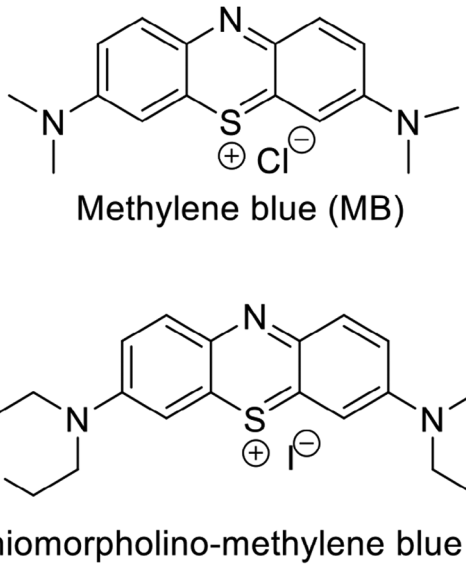

Figure 2. Chemical structures of MB and TMB.

was lower than that of MB. DPBF was mostly degraded in ≈100 s for TMB, whereas for MB, it was < 15 s (Figure 3). The reason for this is likely a reduced triplet state lifetime or a decrease in the ISC quantum yields for TMB, but at this point, no detailed studies were conducted to verify the precise reason. Nevertheless, this difference in $^1O_2$ production is minimal and sufficient enough to be useful and comparable to other popular PS dyes like porphyrin. Substitution of thiomorpholine resulted in significantly enhanced hydrophobicity and water insolubility, thereby enabling the utilization of TMB in the next stage for printing the PPE.

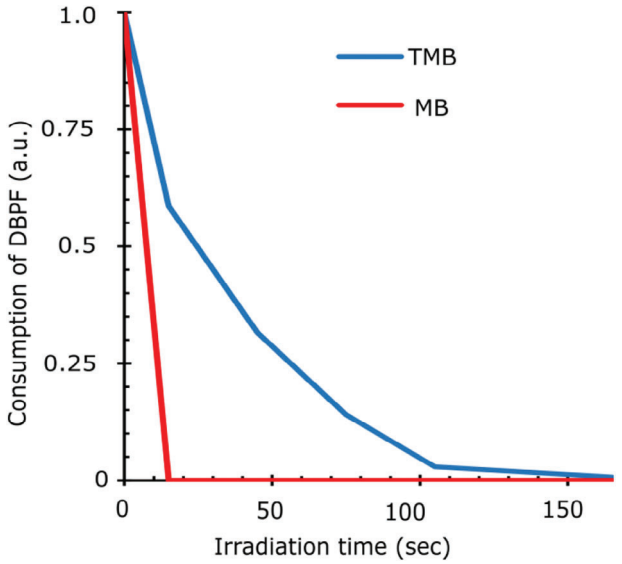

Figure 3. Comparison of the singlet oxygen ($^1O_2$) production rates of methylene blue (MB) and thiomorpholino-methylene blue (TMB) at 20 °C in DMSO with 1,3-diphenylbenzofuran as scavenger. Decay of DPBF was measured at 420 nm by Tecan well plate reader. Irradiation of samples was done at 690 nm, using 128 red LED with an energy of 9.27 ± 0.3 W cm^{-2}.

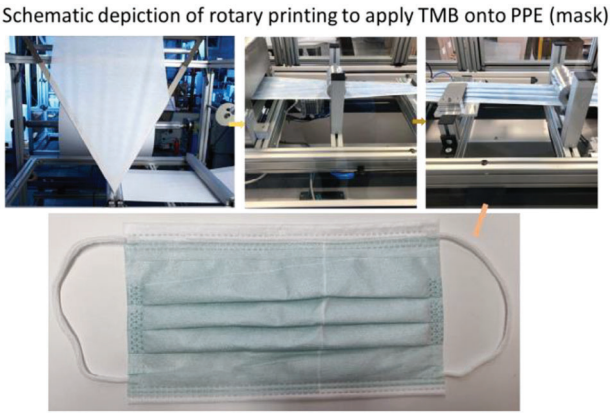

Figure 4. Overview of the process to rotary-print three-layered medical face masks with TMB. The top left image shows bulk textile-role folding to make it ready for printing at one side of surface as in the middle image, and the right image shows shape formation of printed fleece folded into mask; bottom shows TMB-printed mask produced in industrial scale.

To facilitate the rotary printing of TMB onto the masks, a formulation was prepared using the commercially available nitrocellulose-based adhesive agent MigraStar GS (MG, supplied by J+S-Druckfarben, Höver, Germany). TMB was added in different concentrations, from 0.5% to 5% (w/v) into MG and dissolved it by mechanical stirring. The formed suspension was used in a printing process on an industrial rotary printing system for textiles (**Figure 4**).

The resulting printed mask with 5% TMB showed good aesthetic color that mimicked the conventional three-layered blue-pigment printed masks. The coated material was subsequently examined for its pore structure and anti-bacterial activity.

Scanning electron microscopy (SEM) was utilized to exclude changes in the pore structure of masks after being printed with TMB. For the comparisons, masks without any dye (blank), and commercially available blue-pigment printed masks were used. The SEM images revealed that there were no changes in porous structures of the PP-fleece, before and after coating with TMB. The pore size and structure remained unchanged and were indistinguishable from unmodified PP and commercially sold blue-pigment stained PP fibers. It was further observed that the TMB coating formed an ultra-thin film on the surface of the fibers, which is in contrast to commercial blue pigments, being visible as small particles on top of the single fibers (**Figure 5**).

This data was further correlated with EDS measurements and SEM/EDS mapping to verify the success of the applied coating, proof its stability during laundering, abrasion, and tape pealing. EDS showed that the observed spots contain sulfur (S) and iodine (I), in low concentrations, as well as oxygen (O), as well as trace impurities of other elements (see Figures S5–S8, Supporting Information). S and I are core components of the TMB and O is part of the cellulose used in the printing medium. For mapping purposes the concentration of sulfur and iodine was below the detection threshold, oxygen on the other hand could be mapped and the overlay of the SEM and EDS maps show a close correlation between the observed spots in SEM and the oxygen (**Figure 6**). Further, in this study, we tested the dye adhesion efficiency, in laundering, abrasion, or tape peeling of the

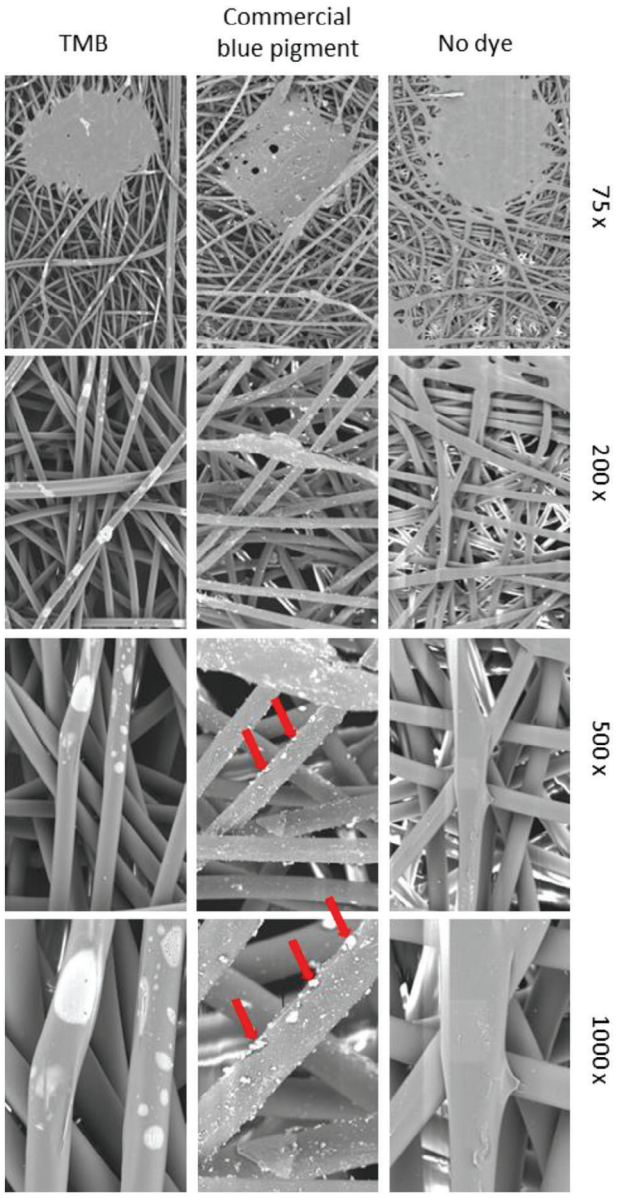

Figure 5. Scanning electron microscopy (SEM) images polypropylene-fleece masks of 5% TMB printed (left column), commercially-used blue pigment stained (middle column) and unmodified (right column), at 75, 200, 500, and 1000 times magnification (red arrows indicate particles in commonly used blue-pigment).

surface. The SEM/EDS of surfaces proved that such mechanical actions did not affect the TMB coating that remains stably attached.

Next, we studied the shear-rate dependent viscosities of the prepared TMB adhesive and compared it with MG alone. The shear-rate dependent viscosities (η) of the prepared TMB formulations in MG adhesive were measured at 22 °C using a stress-controlled DHR-3 rheometer (TA Instruments) equipped with a 40 mm/1° cone-plate geometry (**Figure 7**). MG alone served as control. The shear rate ($\dot{\gamma}$) was increased from 10^{-1} to 10^{3} s^{-1}, with a measurement time of 30 s at each shear rate. TMB in

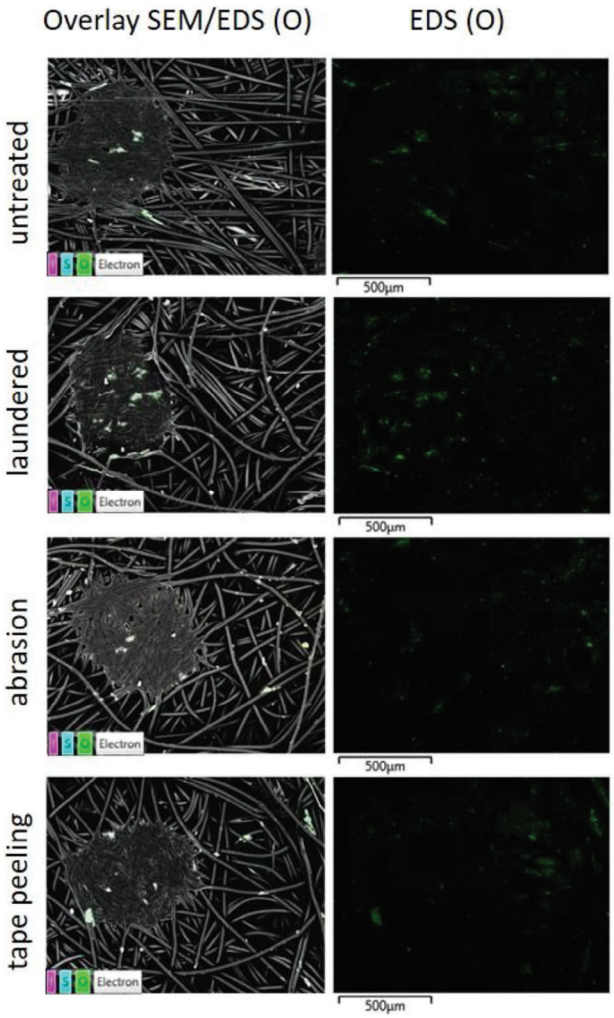

Figure 6. SEM/EDS mapping of the applied antimicrobial coating before and after application of laundering, abrasion and tape peeling; sulfur and iodine are not visible due to their low concentrations, oxygen (green) stems from the nitrocellulose based printing medium.

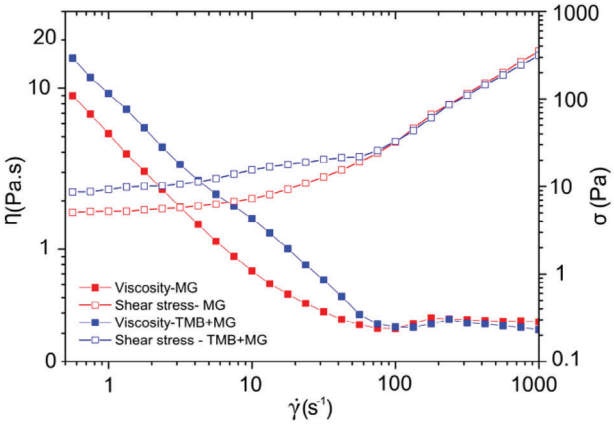

Figure 7. Flow curves flow curves with 5% of TMB in Migrastar GS and neat Migrastar GS.

Table 1. Breathability (DP) and bacterial filtration efficiency (BFE) results obtained from uncoated (no-dye), TMB-coated, and commercial blue-pigmented facemasks. Data are presented as mean±standard deviation of five replicated measurements for each mask model.

Mask type	DP [Pa/cm^2]	BFE [%]
TMB coated	31.0±1.1	99.93±0.05
Commercial blue pigment	29.1±1.7	99.90±0.09
No dye	31.2±0.6	99.95±0.03

adhesive showed strong shear-thinning behavior at low shear rates (up to ≈10 s^{-1}), while a Newtonian plateau was observed at high shear rates (>100 s^{-1}). The TMB dye embedding induced a slight difference in viscosity of the MG (from 5.21 to 9.27 at 1 s^{-1}, from 0.73 to 1.54 at 10 s^{-1}), but the viscosities at the lowest to highest shear rates were almost identical. Furthermore, it was observed that the samples MG and TMB+MG exhibited yield stress, characterized by constant shear stress in the low shear rate region. This means that the materials exhibit solid-like behavior (i.e., they do not flow) under small stresses. The embedding of TMB in MG led to a marginal increase in the yield stress from ≈5 Pa to ≈8 Pa, suggesting only a minimal effect on the MG upon dye embedding. In conclusion, the embedding of TMB dye into commercial adhesive MG did not induce significant changes in the viscosity, thereby permitting the use of TMB dye formulations in industrial rotary printing devices. Results of breathability (DP, Pa/cm^2) and bacterial filtration efficiency (BFE, %) measurements (Figures S1–S3, Supporting Information) showed no impact of TMB coating on mask's performance (**Table 1**, **Figure 8**) compared to uncoated masks.

To assess the antimicrobial properties, a modified procedure leaning on ISO norm 20 743 was used. Bacterial germ solution (1.0 – 3.0 $^{*}\cdot 10^5$ CFU mL^{-1}) was seeded on the sterilized textile surface. The seeded surfaces were then exposed to a 1600 lumen white light (commercially sold by OSRAM, as warm white lighting) source placed at a distance of 15 cm, to the textile for 6 to 24 h at 37 °C. Subsequently, the bacteria present on the fleece were collected by using ultrasound and vortex, and seeded on agar plates (in 1:200 dilution). The plates were incubated for 24 h

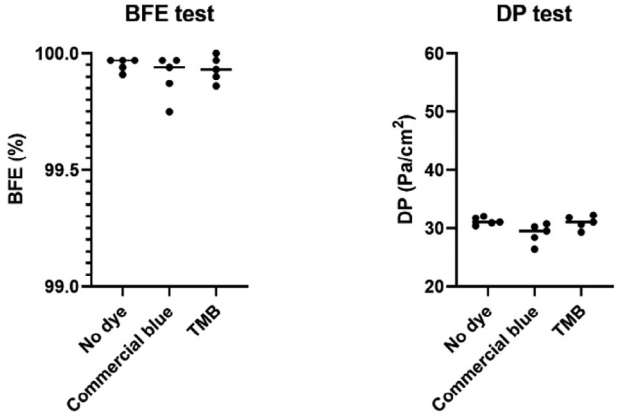

Figure 8. Results of BFE (left) and DP (right) test performed on uncoated (no-dye), commercial blue pigmented, and TMB-coated face masks.

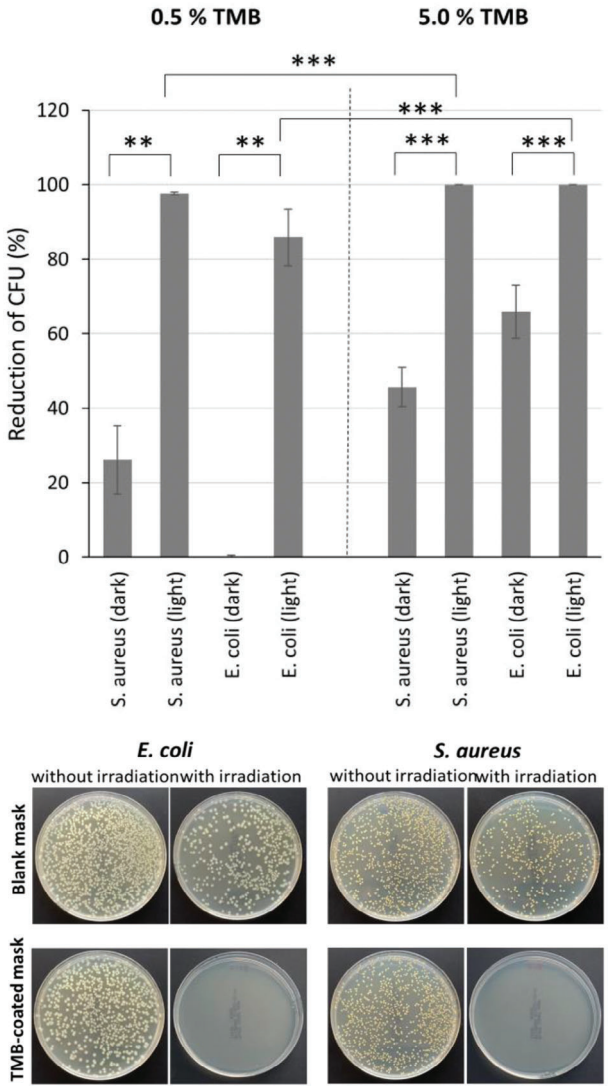

Figure 9. Top: Graphical representation of reduction in bacterial colony forming units, with and without TMB coating and with/without light irradiation. Bottom: Images of bacterial colonies, of the bacteria seeded on the facemasks uncoated/coated with 5% TMB-Migrastar, collected after with/without irradiation.

and the number of colony-forming units (CFU) was determined by counting the colonies (**Figure 9**). The antimicrobial efficiency was quantified as the difference in CFU from test material over blank control and non-irradiated materials (see Supporting Information for the detailed protocol).

The results confirmed that 0.5% TMB in MG was not sufficient to generate sufficient antimicrobial activity, as the reduction of CFU was only ≈85.85 ± 7.62% and 97.63 ± 0.42% for *E. coli* and *S. aureus*, respectively. Increasing the TMB concentration to 5.0% in MG solved this issue, and resulted in strongly antimicrobial surfaces. The tested Gram-positive and negative strain showed a reduction of >99.99% in CFU within 6 h, proving that the TMB-based LAMM material is suitable for practical application in PPEs (**Table 2**).

Table 2. Antibacterial properties of TMB (0,5 and 5,0%) coated masks toward E. coli and S. aureus strains after irradiation with 1600 lumen white light lamps, from 15 cm distance to the mask.

	% of reduction in CFU			
Test strain	0.5% TMB		5.0% TMB	
	PDT for 24 h		PDT for 6 h	
	with light	*w/o light*	*with light*	*w/o light*
E. coli	85.85%	0.21%	99.99+ %	65.90%
S. aureus	97.63%	26.14%	99.99+ %	45.71%

3. Conclusion

In conclusion, we presented a simple and industrially transferable method to minimize plastic-waste produced by personal protective equipment (PPE) using existing technologies and methods. This method used a routinely applied rotary printing method with nitrocellulose adhesive (Migrastar) matrix, and a photodynamic antimicrobial agent, thiomorpholino-methylene blue (TMB) for coating of PP fleece. The TMB upon photo excitation under standard household white light continuously generates $^1O_2$ from $^3O_2$, which has a short lifetime and high reactivity. A concentration of 5% TMB (w/w) in Migrastar was found to be suitable for coating of PPEs with the industrial rotary printing process. The coated PPE eradicated > 99.99% of Gram-negative *E. coli* and Gram positive *S. aureus* at the PPE surface, as well as provided a visually aesthetic color. Further, SEM/EDS measurements showed that the coating formed a thin and spotty layer on the PPE surface that was stable toward laundering and abrasion. Most notably the TMB coating did not influence the breathability and filtration efficiency of masks compared to uncoated masks. Overall, the here presented work proves that extended use of PPE items is possible without hampering safety and efficacy, and can thus contribute to the reduction of plastic waste associated with PPEs.

4. Experimental Section

Reagents and solvents were procured from Chempur, Acors Organics, Merck-Sigma–Aldrich, and VWR, and used as obtained toward the TMB synthesis. Migrastar GS was obtained from J+S Druckfarben, Germany. Polypropylene fleece and printing equipment were provided by Ultratex GmbH in Aachen. Antimicrobial tests were conducted at the MTC Brünke. For details, please refer to Electronic Supporting Information (ESI).

BFE and DP tests were conducted on uncoated (no-dye), TMB-coated, and commercial blue-pigmented face masks according to European Standard EN 14 683:2019+AC[37] using test rigs previously detailed and validated.[38,39]

Supporting Information

Supporting Information is available from the Wiley Online Library or from the author.

Acknowledgements

The financial support from the Zentrale Innovation Mittelstand (ZIM) initiative to the project AVSchutz (KK5006902SK0) of the German federal government (BMWK) is gratefully acknowledged. The SEM/EDX imaging by Electron Microscopy Core Facility of RWTH Aachen (Dr. A. Schwedt, F. Mariano) is gratefully acknowledged. F.T. holds a fixed-term researcher position supported by the European Union, FSE-REACT-EU, Programma Operativo Nazionale, Azione IV.4 – Research and Innovation, DM 641 1062/2021, which is kindly acknowledged.

Open access funding enabled and organized by Projekt DEAL.

Conflict of Interest

The authors declare no conflict of interest.

Data Availability Statement

The data that support the findings of this study are available in the supplementary material of this article.

Keywords

antimicrobial face masks, antimicrobial photodynamic effect, reactive oxygen species, self-disinfecting polymers, visible light active photosensitizer

Received: July 18, 2023
Revised: October 13, 2023
Published online: December 19, 2023

[1] A. A. G. Carvalho, A. L. E. S. Aidar, B. C. D. Santos, D. A. B. Kuramoto, M. R. Pereda, R. M. Correia, L. C. U. Nakano, J. E. Amorim, *J Vasc Bras* **2021**, *20*, https://doi.org/10.1590/1677-5449.200044.
[2] J. H. Verbeek, B. Rajamaki, S. Ijaz, R. Sauni, E. Toomey, B. Blackwood, C. Tikka, J. H. Ruotsalainen, F. S. Kilinc Balci, *Cochrane Database Syst Rev* **2020**, *4*, CD011621.
[3] L. D. Nghiem, H. M. N. Iqbal, J. Zdarta, H. M. N. Iqbal, J. Zdarta, *Case Stud Chem Environ Eng* **2021**, *4*, 100125.
[4] S. I. AgileIntel Research (ChemIntel360). Statista, "Market Volume of Polypropylene Worldwide from 2015 to 2021, with a Forecast for 2022 to 2029 (in Million Metric Tons).," can be found under https://www.statista.comstatistics/1245169/polypropylene-market-volume-worldwide/, (accessed: March 2023).
[5] Y. Peng, P. Wu, A. T. Schartup, Y. Zhang, Proc. Natl. Acad. Sci **2021**, *118*, e2111530118.
[6] J. C. Prata, A. L. P. Silva, T. R. Walker, A. C. Duarte, T. Rocha-Santos, *Environ. Sci. Technol.* **2020**, *54*, 7760.
[7] C. Schweitzer, R. Schmidt, *Chem. Rev.* **2003**, *103*, 1685.
[8] M. S. Baptista, J. Cadet, P. Di Mascio, A. A. Ghogare, A. Greer, M. R. Hamblin, C. Lorente, S. C. Nunez, M. S. Ribeiro, A. H. Thomas, M. Vignoni, T. M. Yoshimura, *Photochem. Photobiol.* **2017**, *93*, 912.
[9] D. Sanders, A. Grunden, R. R. Dunn, *Biol Lett* **2021**, *17*, rsbl.2020.0700.
[10] T.-L. Su, T.-P. Chen, J. F. Liang, *Colloids Surfaces A Physicochem. Eng. Asp.* **2023**, *657 (part A)*, 130506.
[11] J. J. Richardson, W. Liao, J. Li, B. Cheng, C. Wang, T. Maruyama, B. L. Tardy, J. Guo, L. Zhao, W. Aw, H. Ejima, *Sci. Rep.* **2022**, *12*, 2071.
[12] J. Srour, E. Berg, B. Mahltig, T. Smolik, A. Wollenberg, *J. Eur. Acad. Dermatology Venereol.* **2019**, *33*, 384.
[13] R. Nawab, A. Iqbal, F. Niazi, G. Iqbal, A. Khurshid, A. Saleem, M. F. H. Munis, *Polym. Bull.* **2022**, *80*, 7221.
[14] M. S. Hassan, M. K. Attia, R. Attia, *J Ind Text* **2022**, *52*, 152808372211198.
[15] I. Masłowska-Lipowicz, A. Słubik, *J. Text. Inst.* **2022**, *9*, 095303.

[16] M. F. Tahir, M. Z. Khan, S. Attacha, N. Asim, M. Tayyab, A. Ali, J. Militky, B. Tomková, *Nanomaterials* **2022**, *12*, 3629.
[17] P. Prabhakar, R. K. Sen, M. Patel, Shruti, N. Dwivedi, S. Singh, P. Kumar, M. Chouhan, A. K. Yadav, D. P. Mondal, P. R. Solanki, A. K. Srivastava, C. Dhand, *Colloids Surf., B* **2022**, *220*, 112913.
[18] N. Chowdhury, G. M. Faysal, R. Saha, A. Shikder, *J. Nat. Sci. Text. Technol.* **2022**, *1*, 69.
[19] S. Li, X. Lin, S. Gong, *Cellulose* **2022**, *29*, 7397.
[20] P. Wang, M. Zhang, J. Qu, L. Wang, J. Geng, F. Fu, X. Liu, *Cellulose* **2022**, *29*, 3569.
[21] J. Chen, W. Wang, P. Hu, D. Wang, F. Lin, J. Xue, Z. Chen, Z. Iqbal, M. Huang, *Dye. Pigment.* **2017**, *140*, 236.
[22] F. Jin, S. Liao, Q. Wang, H. Shen, C. Jiang, J. Zhang, Q. Wei, R. A. Ghiladi, *Appl. Surf. Sci.* **2022**, *587*, 152737.
[23] M. A. Castriciano, R. Zagami, M. P. Casaletto, B. Martel, M. Trapani, A. Romeo, V. Villari, M. T. Sciortino, L. Grasso, S. Guglielmino, L. M. Scolaro, A. Mazzaglia, *Biomacromolecules* **2017**, *18*, 1134.
[24] A. Schlachter, P. Asselin, P. D. Harvey, *ACS Appl. Mater. Interfaces* **2021**, *13*, 26651.
[25] J. Chen, L. Yang, J. Chen, W. Liu, D. Zhang, P. Xu, T. Dai, L. Shang, Y. Yang, S. Tang, Y. Zhang, H. Lin, Z. Chen, M. Huang, *Chem. Eng. J.* **2019**, *374*, 1373.
[26] S. B. Jeong, D. U. Lee, B. J. Lee, K. J. Heo, D. W. Kim, G. B. Hwang, A. J. Macrobert, J. H. Shin, H. S. Ko, S. K. Park, Y. S. Oh, S. J. Kim, D. Y. Lee, S.-B. Lee, I. Park, S. B. Kim, B. Han, J. H. Jung, D. Y. Choi, *Chem. Eng. J.* **2022**, *440*, 135830.
[27] C. R. Ghareeb, B. S. T. Peddinti, S. C. Kisthardt, F. Scholle, R. J. Spontak, R. A. Ghiladi, *Front Med* **2021**, *8*, https://doi.org/10.3389/fmed.2021.657837.
[28] H. Wang, G. W. Wagner, A. X. Lu, D. L. Nguyen, J. H. Buchanan, P. M. Mcnutt, C. J. Karwacki, *ACS Appl. Mater. Interfaces* **2018**, *10*, 18771.
[29] L. Zhu, Y. Liu, X. Ding, X. Wu, W. Sand, H. Zhou, *RSC Adv.* **2019**, *9*, 17726.
[30] M. Arenbergerova, P. Arenberger, M. Bednar, P. Kubat, J. Mosinger, *Exp Dermatol* **2012**, *21*, 619.
[31] K. H. Hong, G. Sun, *J. Appl. Polym. Sci.* **2009**, *112*, 2019.
[32] J. Clifton, J. B. Leikin, *Am. J. Ther.* **2003**, *10*, 289.
[33] J. P. Tardivo, A. Del Giglio, C. S. De Oliveira, D. S. Gabrielli, H. C. Junqueira, D. B. Tada, D. Severino, R. De Fátima Turchiello, M. S. Baptista, *Photodiagnosis Photodyn Ther* **2005**, *2*, 175.
[34] L. S. De Moraes, D. Edwards, A. J. Florence, A. Johnston, B. F. Johnston, C. A. Morrison, A. R. Kennedy, *Cryst. Growth Des.* **2017**, *17*, 3277.
[35] A. Delport, B. H. Harvey, A. Petzer, J. P. Petzer, *ACS Chem. Neurosci.* **2018**, *9*, 2917.
[36] E. L. Rosenthal, *J Nucl Med* **2014**, *55*, 1893.
[37] European Committee for Standardization, European Standard EN 14683:2019+AC Medical face masks – Requirements and test methods **2019**.
[38] F. Tessarolo, G. Nollo, D. Maniglio, M. Rigoni, L. Benedetti, F. Helfer, I. Corradi, L. Rovati, A. Ferrari, M. Piccini, L. Accorsi, E. Veronesi, A. Cuoghi, S. Baglio, N. Tuccitto, S. Stefani, S. Stracquadanio, F. Caraci, A. Terrasi, A. Tricomi, M. Musumeci, A. Miraglia, G. Cuttone, S. Cosentino, C. Muscas, L. A. Vitali, D. Petrelli, L. Angrisani, R. Colicchio, A. D'anna, et al., *Int J Environ Res Public Health* **2021**, *18*, 1462.
[39] F. Tessarolo, G. Nollo, L. Benedetti, F. Helfer, L. Rovati, A. Ferrari, G. Marchetti, F. Reverberi, S. Baglio, N. Tuccitto, S. Stefani, S. Stracquadanio, F. Caraci, A. Terrasi, A. Tricomi, M. Musumeci, A. Miraglia, G. Cuttone, S. Cosentino, L. Agostino Vitali, D. Petrelli, S. Ilaria Ciancia, M. Mingoia, P. Castellini, S. Simoni, L. Montalto, A. Baleani, P. Chiariotti, N. Paone, *Measurement* **2021**, *189*, 110481.